

ASTR 610

Theory of Galaxy Formation

Lecture 20: Numerical Simulations

FRANK VAN DEN BOSCH
YALE UNIVERSITY, FALL 2020



Numerical Simulations

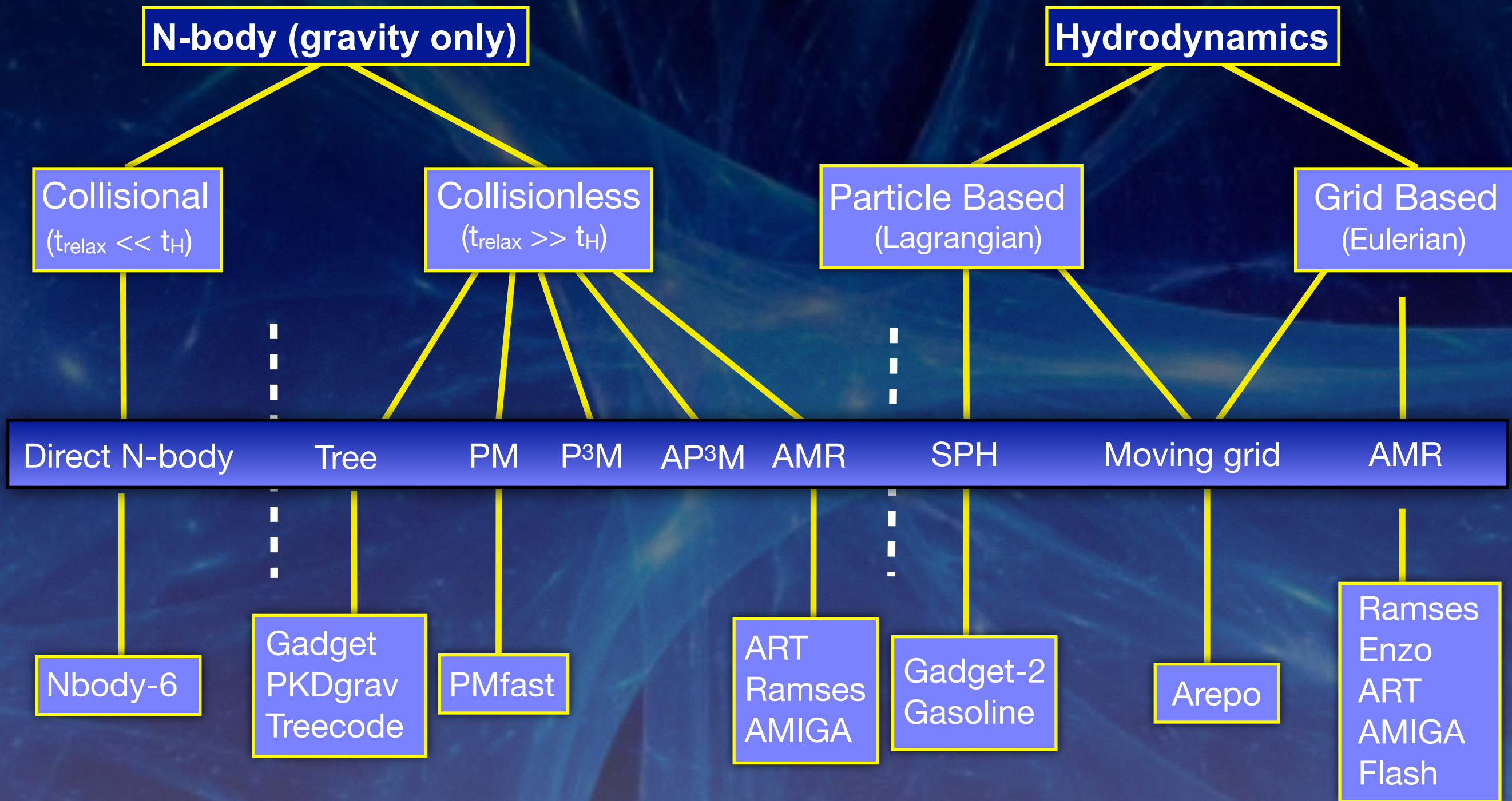
In this lecture we discuss the various methods that are used in N-body simulations of structure formation. Due to time constraints we will mainly focus on pure N-body (gravity only) simulations.

Topics that will be covered include:

- Overview of Simulations Codes
- N-Body methodology
- Force Calculation
- Time Integration
- Force Softening
- Relaxation Processes

Parts of this lecture are copied from an excellent lecture by Joshua Barnes.

Overview of Simulation Method & Codes*



*NOTE: this overview is by no means exhaustive!!

Collisionless Dynamics

The equations governing a collisionless system are the Vlasov-Poisson equations:

$$\rho(\vec{x}, t) = \int d\vec{v} f(\vec{x}, \vec{v})$$

$$\Phi(\vec{x}, t) = -G \int d\vec{x}' \frac{\rho(\vec{x}', t)}{|\vec{x} - \vec{x}'|}$$

Poisson eq.

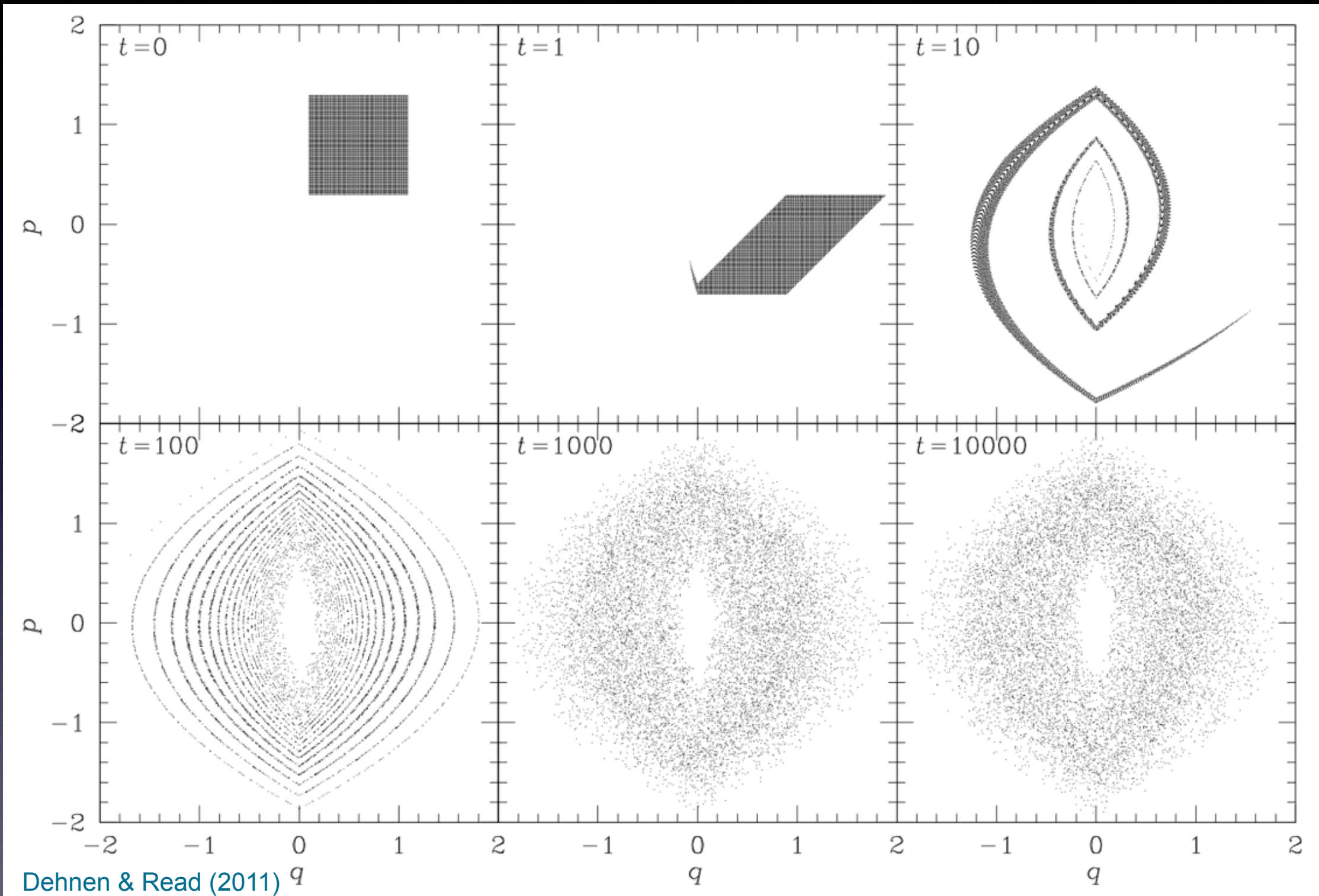
$$\frac{df}{dt} = \frac{\partial f}{\partial t} + \vec{v} \cdot \frac{\partial f}{\partial \vec{x}} - \frac{\partial \Phi}{\partial \vec{x}} \cdot \frac{\partial f}{\partial \vec{v}} = 0$$

CBE (Vlasov) eq.

The direct numerical solution of the CBE, a non-linear PDE in seven dimensions, is not feasible. The main problems are:

- The 6D grid on which to solve the CBE takes too many cells (for given resolution)
- Under CBE, the DF develops ever stronger gradients; initial fluctuations are not averaged away, but mixed, leading to ever thinner layers of phase-space density.

Mixing in Collisionless systems



Phase-mixing of 10^4 points in simple 1D Hamiltonian. The fine-grained DF is initially either 0 or 1, but at late times a smooth coarse-grained DF develops...

The N-body Methodology

Rather than solving the Vlasov-Poisson equations on a 6D grid, we use Monte-Carlo techniques to solve the equations of motion for a sample of N `bodies'.

Replace smooth DF with N bodies:

$$f(\vec{x}, \vec{v}) \rightarrow \{(m_i, \vec{x}_i, \vec{v}_i) | i = 1, 2, \dots, N\}$$

$$f(\vec{x}, \vec{v}) \simeq \sum_{i=1}^N m_i \delta^3(\vec{x} - \vec{x}_i) \delta^3(\vec{v} - \vec{v}_i)$$

Select (\vec{x}_i, \vec{v}_i) with probability proportional to the DF, and assign all bodies equal mass:

$$m_i = \frac{1}{N} \int d\vec{x} d\vec{v} f(\vec{x}, \vec{v})$$

Advancing Time

Move bodies along phase flow (method of characteristics)

$$(\dot{\vec{x}}_i, \dot{\vec{v}}_i) = (\vec{v}_i, -\nabla\Phi_i)$$

Estimate potential from N-body representation using Poisson equation:

$$\nabla^2\Phi|_{\vec{x}} = 4\pi G \sum_{i=1}^N m_i \delta^3(\vec{x} - \vec{x}_i)$$

This will yield the usual N-body equation for point masses. But, singular potentials are awkward, so we smooth the density field.

$$\delta^3(\vec{x} - \vec{x}_i) \rightarrow \frac{3}{4\pi} \frac{\varepsilon^2}{(|\vec{x} - \vec{x}_i|^2 + \varepsilon^2)^{5/2}}$$

Plummer (1911) smoothing;
See Dehnen+01 for other
smoothing kernels...

This substitution yields the following equations of motion:

$$\frac{d\vec{x}_i}{dt} = \vec{v}_i \quad \frac{d\vec{v}_i}{dt} = \sum_{j \neq i}^N \frac{Gm_j(\vec{x}_j - \vec{x}_i)}{(|\vec{x}_j - \vec{x}_i|^2 + \varepsilon^2)^{3/2}}$$

ε is called the
softening length

Relaxation Time

N-body models **relax** (undergo gravitational ‘collisions’, aka ‘encounters’).
The rate at which this **two-body relaxation** occurs is given by **relaxation time**:

$$t_{\text{relax}} \simeq \frac{N}{8 \ln(R/\varepsilon)} t_{\text{cross}} \quad t_{\text{cross}} \simeq \frac{R}{\sigma_v}$$

Since **N** is typically many orders of magnitude smaller in N-body representation than in real system, relaxation time of simulated system is orders of magnitude smaller than for real system.

Ex: dark matter halo $N_{\text{WIMP}} \sim 10^{70}$, whereas $N_p \approx 10^9$

Ansatz: as long as $t_{\text{relax}} \gg t_H$ (two-body) relaxation shouldn’t be an issue...

NOTE: (artificially short) relaxation time depends only very weakly on **softening length**. Softening is NOT introduced to eliminate relaxation effects; it only suppresses the large-angle ‘scattering’ due to close encounters... For uniform density, each octave in impact parameter contributes equally to relaxation!!!

Force Calculation

Particle-Particle (PP): simply sum over all other bodies

$$\frac{\vec{F}_i}{m_i} = \frac{d\vec{v}_i}{dt} = \sum_{j \neq i}^N \frac{Gm_j(\vec{x}_j - \vec{x}_i)}{(|\vec{x}_j - \vec{x}_i|^2 + \varepsilon^2)^{3/2}}$$

Advantage is that this is robust, accurate and completely general

Disadvantage is that for each particle, it requires a sum over all N bodies, such that cost of computing forces on all particles requires $\mathcal{O}(N^2)$ operations.

This method is far too slow/costly, and therefore rarely used to simulate collisionless systems. However, it is *the* method to simulate collisional systems such as globular clusters or (open) star clusters...

Force Calculation

Particle-Mesh (PM) method:

(Hockney & Eastwood 1988)

- [1] Divide computational box (size L) in grid of N_c^3 meshes of constant size L/N_c
- [2] Compute mass density on mesh using a “Cloud-in-Cell” (CIC) interpolation scheme.

$$\rho(\vec{q}) = \frac{m}{L^3} \sum_{i=1}^N W(\vec{x}_i - \vec{X}_q)$$

q is mesh location

Here $W(r)$ is a (normalized) kernel function. Note that this density is a convolution of particle distribution with kernel function, and so its Fourier transform is equal to product of \tilde{W}_k and FT of particle density distribution.

- [3] Solve for potential on mesh using the Poisson equation (in Fourier Space)

$$-k^2 \phi_{\vec{k}} = 4\pi G \rho_{\vec{k}}$$

Periodic boundary conditions --> FFT

Force per unit mass at grid points: $F_{\vec{k}} = -i\phi_{\vec{k}}\vec{k}$

Force Calculation

Particle-Mesh (PM) method:

(Hockney & Eastwood 1988)

- [4] Compute each particle acceleration using inverse CIC interpolation scheme

$$F(\vec{x}_i) = \sum_{\vec{q}} W(\vec{x}_i - \vec{X}_q) F(\vec{q})$$

- [5] Update each particle velocity according to its acceleration
- [6] Update each particle position according to its velocity

Advantages:

Fast; computational cost for force calculation only $\mathcal{O}(N)$
Consequently, large numbers of particles can be used

Disadvantages:

Choice of kernel function is non-trivial and can affect numerical accuracy
Force resolution is limited by size of mesh. Large N_c required for accuracy
As clustering develops, forces become less and less accurate

Force Calculation

Particle-Particle-Particle-Mesh (P^3M) method:

(e.g. Efstathiou 1985)

pronounce: P-cube-M

P^3M combines the advantages of **PP** and **PM** methods:

long-range forces ($d \approx 2 L/N_c$) are computed using **PM** (fast)

short-range forces ($d \approx 2 L/N_c$) are computed using **PP** (accurate)

If particles are not strongly clustered, most particle pairs are solved using **PM**
Once particles become strongly clustered, code becomes effectively **PP**.

This problem can be avoided with the use of adaptive sub-meshes; **AP P^3M**

(e.g. Couchman 1991)

With sufficiently adaptive grid, forces on all particles can be computed on a grid, in which case the code becomes essentially an **AMR** (adaptive mesh refinement) code. Different **AMR** codes (e.g., ART, AMIGA, RAMSES) mainly differ in how refinement is handled....

Force Calculation

Tree-Algorithm

Long-range gravitational field dominated by monopole term:

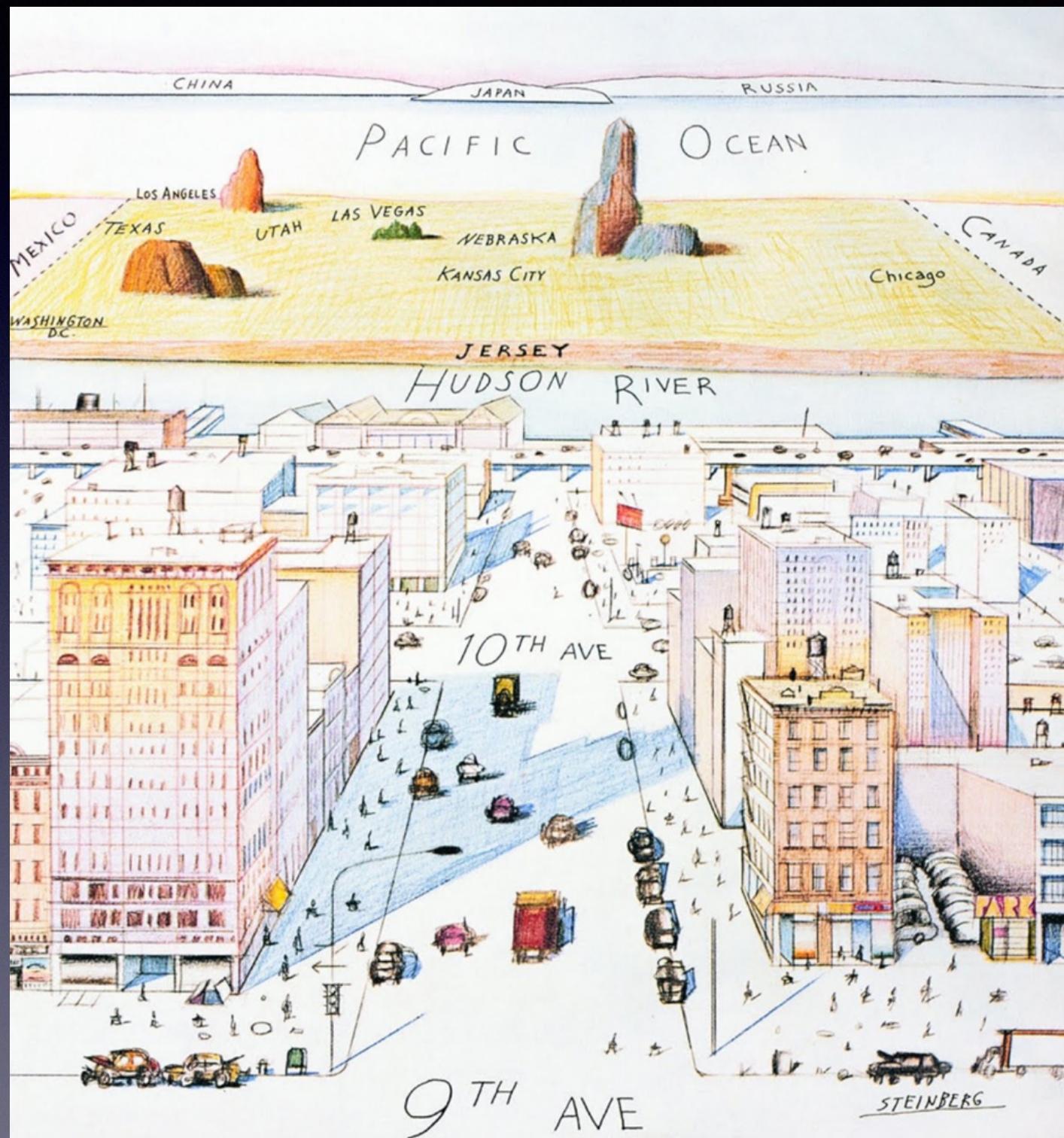
$$\Phi \simeq -\frac{Gm}{r} + \mathcal{O}(r^{-3})$$

→ Group particles according to distance from particle under consideration.

Most efficient way to do this, such that one can use same structure for each particle, is via a 'tree-structure'.

Force from each group is then replaced by its multipole expansion; since higher-order terms die off faster with distance, one only needs to keep lowest order terms (typically up to quadrupole or hexadecapole)

(e.g. Barnes & Hut, 1986)



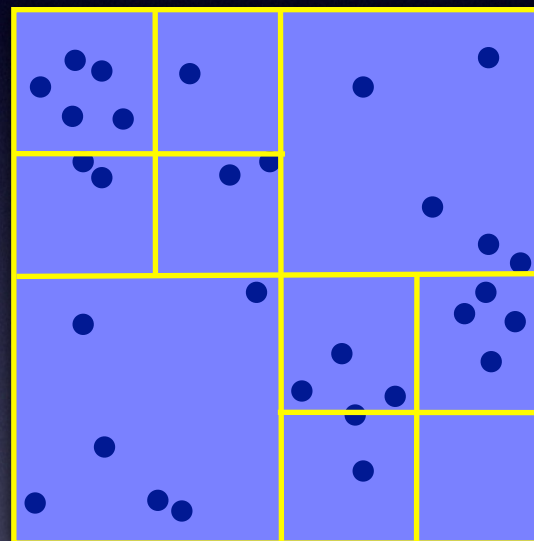
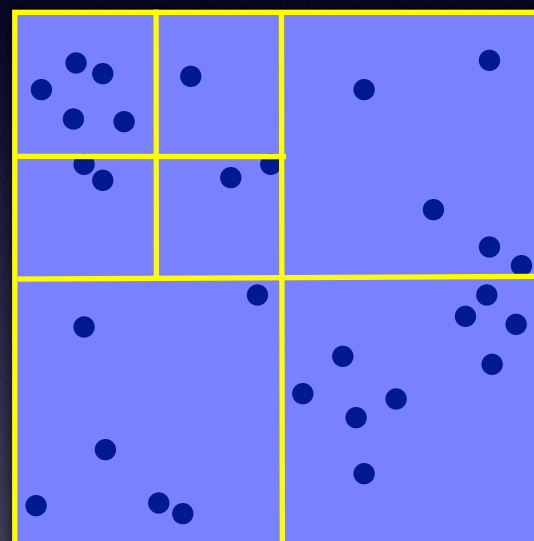
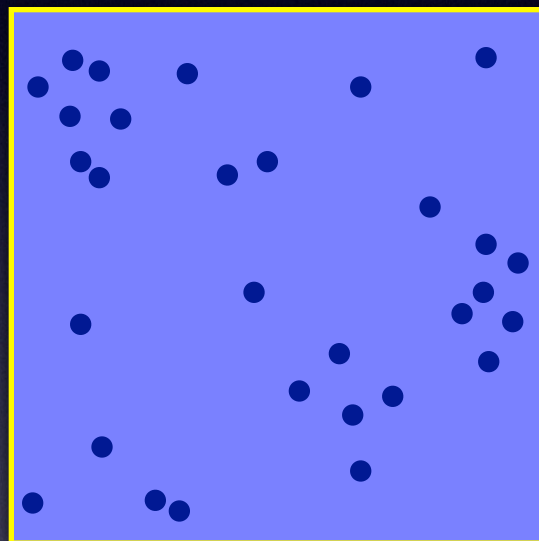
Force Calculation

Tree-Algorithm

(e.g. Barnes & Hut, 1986)

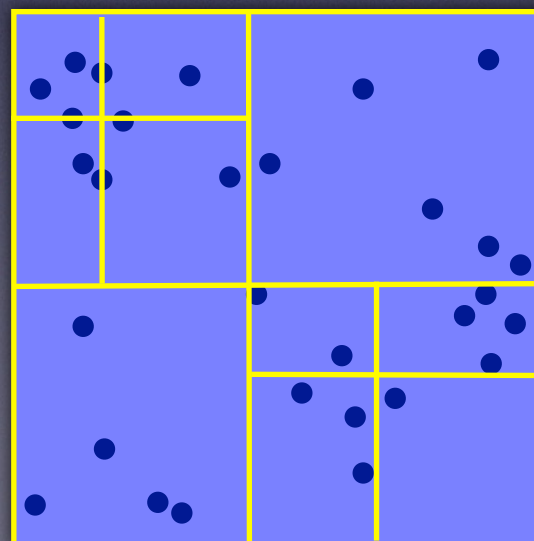
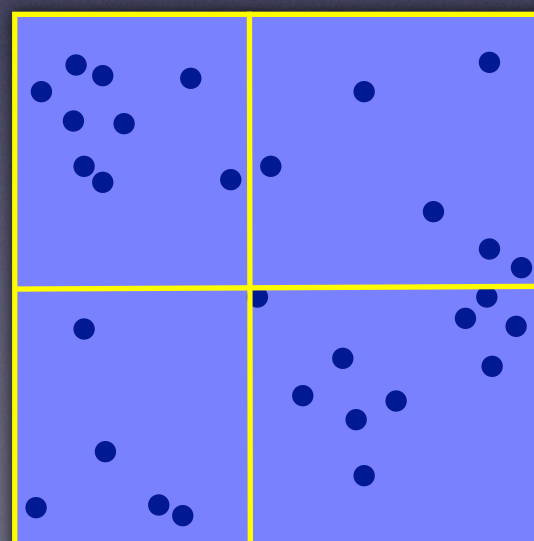
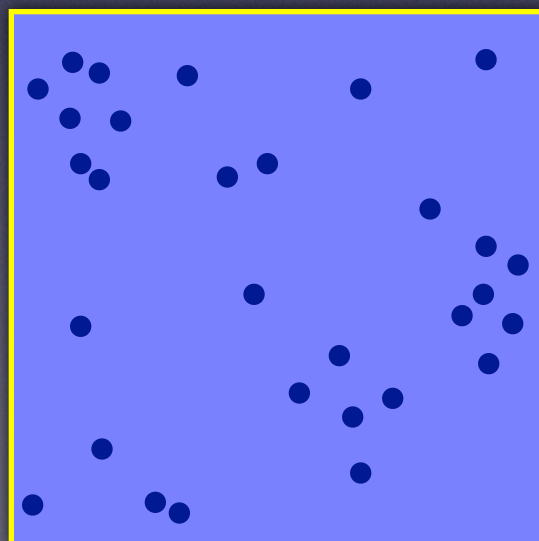
In a tree-code one replaces the sum over N bodies with a sum over $N_c \simeq \mathcal{O}(\log N)$ cells. Hence computational cost of force calculations is $\mathcal{O}(N \log N)$

Different tree-codes use different tree-structures



Octree:

each refinement, cell sizes are cut in half, such that one cell becomes 8 equal-volume cells (e.g., treecode)



kd-tree:

each refinement, cells are divided at median along the x, y, and z axes.
(e.g., PKDgrav)

Force Calculation

Tree-Algorithm

(e.g. Barnes & Hut, 1986)

In a tree-code one replaces the sum over N bodies with a sum over $N_c \simeq \mathcal{O}(\log N)$ cells. Hence computational cost of force calculations is $\mathcal{O}(N \log N)$

In order to compute the force on particle i , one proceeds as follows.

LOOP over all cells of the lowest refinement level.

IF $|\vec{x}_i - \vec{x}_c| > l_c/\theta$ THEN

compute force due to this cell (using low-order multipole expansion)

ELSE

sum the contributions of its sub-cells

END IF

Here \vec{x}_c is the center of mass of the cell, l_c is the size of the cell, and θ is a free parameter, called the opening-angle (typically $\theta \simeq 0.6 - 1.0$).

Smaller θ results in more accurate forces, but at increased CPU cost

Self-Consistent Field Method

(Hernquist & Ostriker 1992)

Represent potential and density as linear sums of basis functions:

$$\Phi(\vec{x}) = \sum_k A_k \Phi_k(\vec{x}) \quad \rho(\vec{x}) = \sum_k A_k \rho_k(\vec{x})$$

Here A_k are coefficients and the basis functions Φ_k and ρ_k are bi-orthogonal and satisfy the Poisson equation:

$$I_k \delta_{kk'} = \int d\vec{x} \rho_k(\vec{x}) [\Phi_{k'}(\vec{x})]^* \quad \nabla^2 \Phi_k = 4\pi G \rho_k$$

The coefficients are computed using:

$$A_k = \frac{1}{I_k} \int d\vec{x} \rho(\vec{x}) [\Phi_k(\vec{x})]^* = \frac{1}{I_k} \sum m_i [\Phi_k(\vec{x}_i)]^*$$

The cost of calculating forces on all bodies is just $\mathcal{O}(N)$

Orbits are integrated in smooth potential; no softening required!

Method can only be used if useful set of basis functions can be found, which is typically only the case for highly symmetric systems....

Time Integration

Once you know the forces, you need to integrate the equations of motion forward in time. Various time-integration methods are employed.

We begin by considering the simple ‘Euler method’ for a time step Δt

$$\vec{x}_i^{[n+1]} = \vec{x}_i^{[n]} + \vec{v}_i^{[n]} \cdot \Delta t$$
$$\vec{v}_i^{[n+1]} = \vec{v}_i^{[n]} + \vec{a}_i^{[n]} \cdot \Delta t$$

simple, but poor accuracy $\mathcal{O}(\Delta t^2)$

NOTE: Euler method is simply based on first-order Taylor series expansion..

We can improve on accuracy by using a higher-order integration scheme.

Second-order Leapfrog Integrator

$$\vec{v}_i^{[n+1/2]} = \vec{v}_i^{[n]} + \frac{1}{2} \vec{a}_i^{[n]} \cdot \Delta t$$
$$\vec{x}_i^{[n+1]} = \vec{x}_i^{[n]} + \vec{v}_i^{[n+1/2]} \cdot \Delta t$$
$$\vec{v}_i^{[n+1]} = \vec{v}_i^{[n+1/2]} + \frac{1}{2} \vec{a}_i^{[n+1]} \cdot \Delta t$$

accuracy $\mathcal{O}(\Delta t^3)$

this integration scheme is sometimes called KDK, for Kick-Drift-Kick

Time Integration

The second-order leapfrog integrator is **symplectic**. This means that it exactly solves an approximate Hamiltonian, which implies that numerical time evolution is a canonical map preserving certain conserved quantities exactly.

Consequently, **leapfrog integrator** is more stable than other (non-symplectic) integrators. It is the most commonly used integrator for collisionless systems.

In principle, one may combine as many kick and drift operations as desired to raise order of integration scheme. However, it is impossible to go beyond second order without having some terms be negative (corresponding to **backwards** integration). This is problematic when variable time steps are required....

See Dehnen & Read (2011) for a more details

The Choice of Time Step

Given the enormous range of dynamical times involved in typical simulations, it has become essential to use **variable time step schemes**:

Most of these adopt a hierarchy of time steps organized in powers of two:

$$\Delta t_n = \Delta t_0 / 2^n$$

n is called the **rung** of the time step

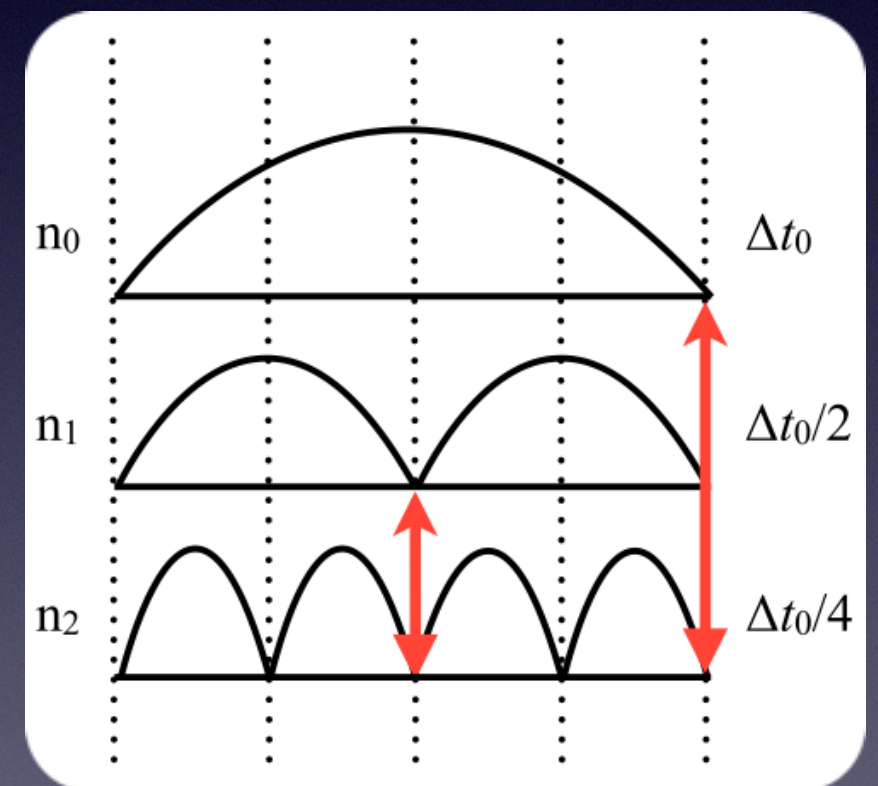
Particles can move to higher rung (smaller time step) whenever they like (meet **time step criterion**), but they may only move to lower rung at **synchronisation points** (red arrows in figure). Resulting asymmetry brakes **symplectic** nature of integrator...

Fixed time step is more accurate, but often too costly...

An often used **time step criterion** is the following

$$\Delta t_i < \eta \sqrt{\varepsilon / |\vec{a}_i|}$$

η free parameter (dimensionless)
 ε softening length



Not well motivated (only on dimensional grounds); many alternatives exist, and most codes allow multiple choices...

Cosmological N-body Simulations

N-body simulations are used to study non-linear dynamical evolution:

Over the years, they have been used to

- study large scale structure (vindication of CDM model)
- probe evolution of non-linear, matter power spectrum
- establish a universal (NFW) density profile of CDM halos
- predict/quantify substructure of dark matter halos
- predict/quantify mass/velocity function of CDM halos

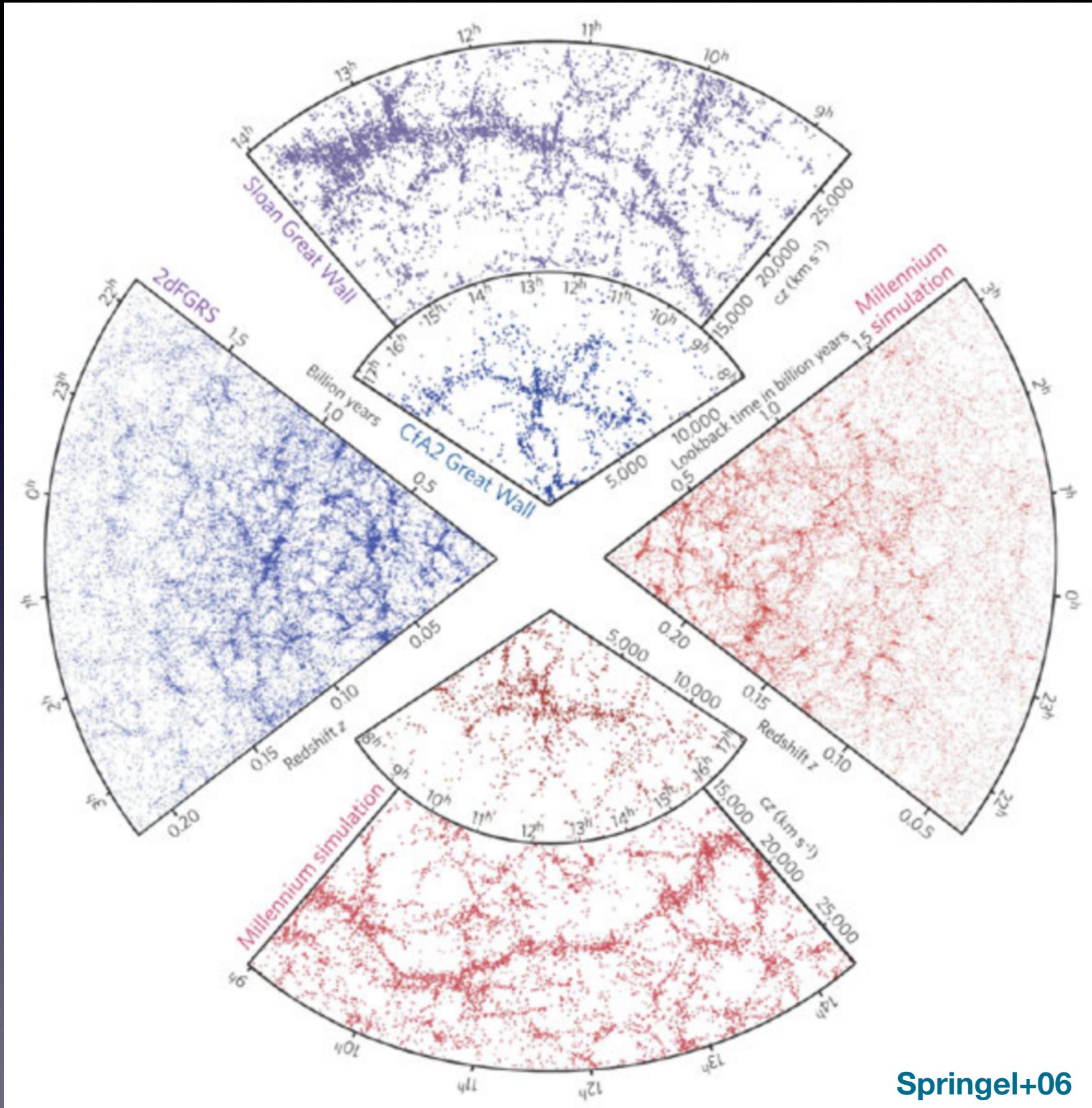
N-body simulations are routinely used as prime tool to address fundamental questions in astrophysics:

- nature of dark energy (determine growth rate of structures)
- nature of dark matter (determines small-scale structure)

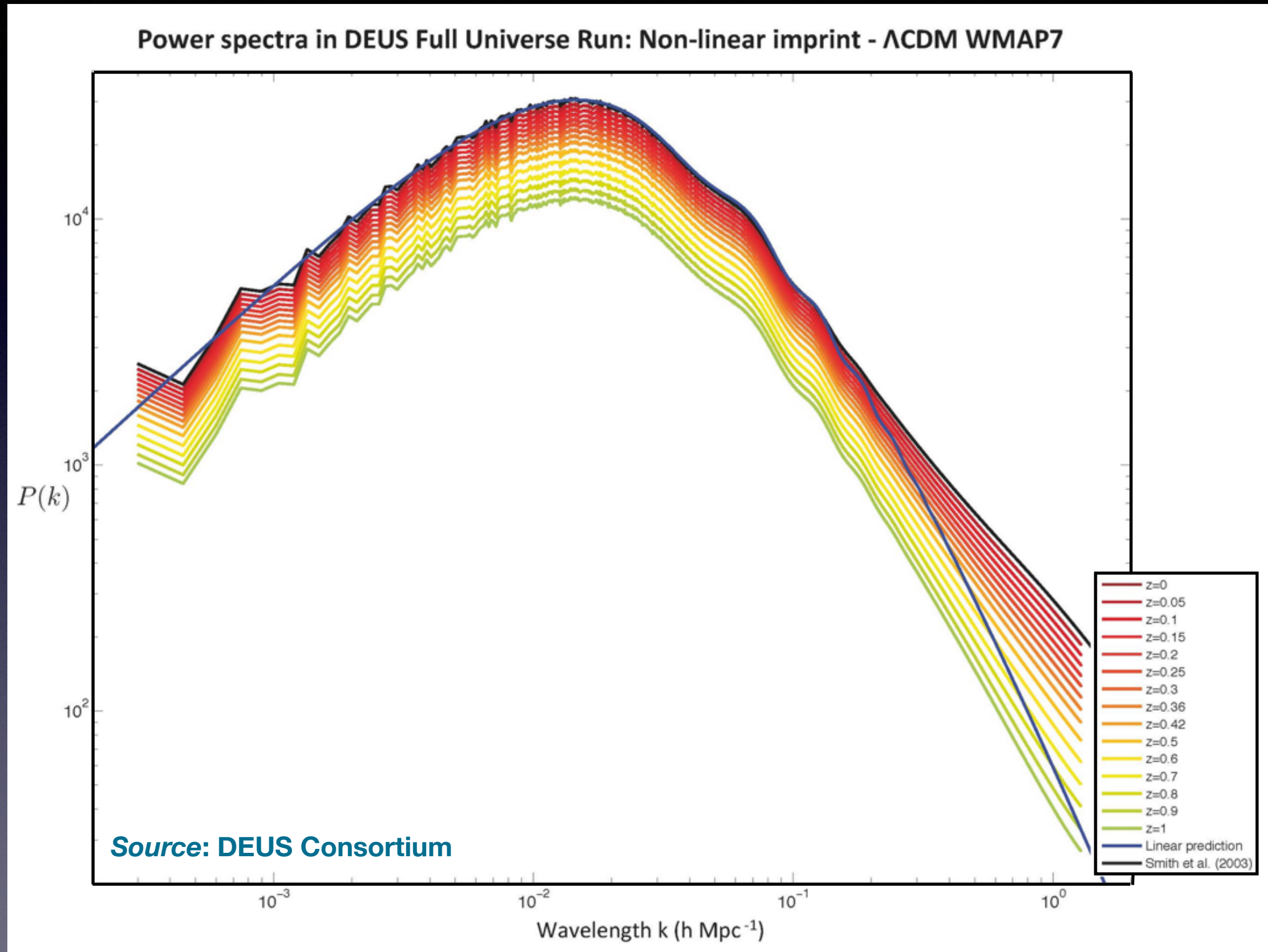
It is crucial that we continue to scrutinize simulations



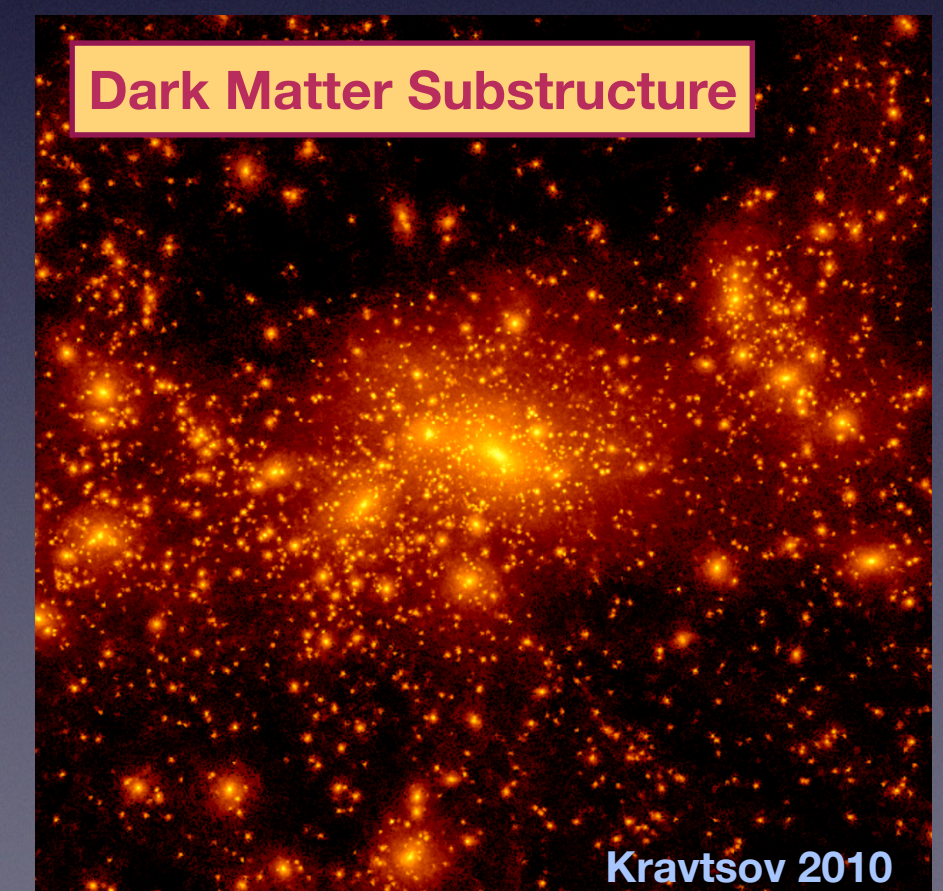
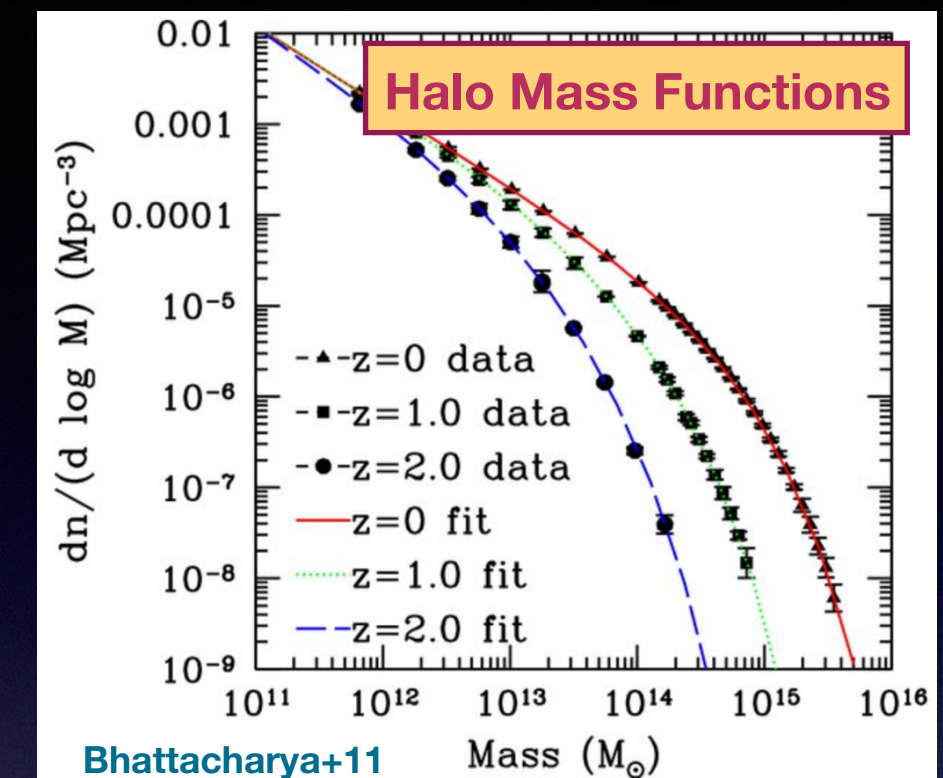
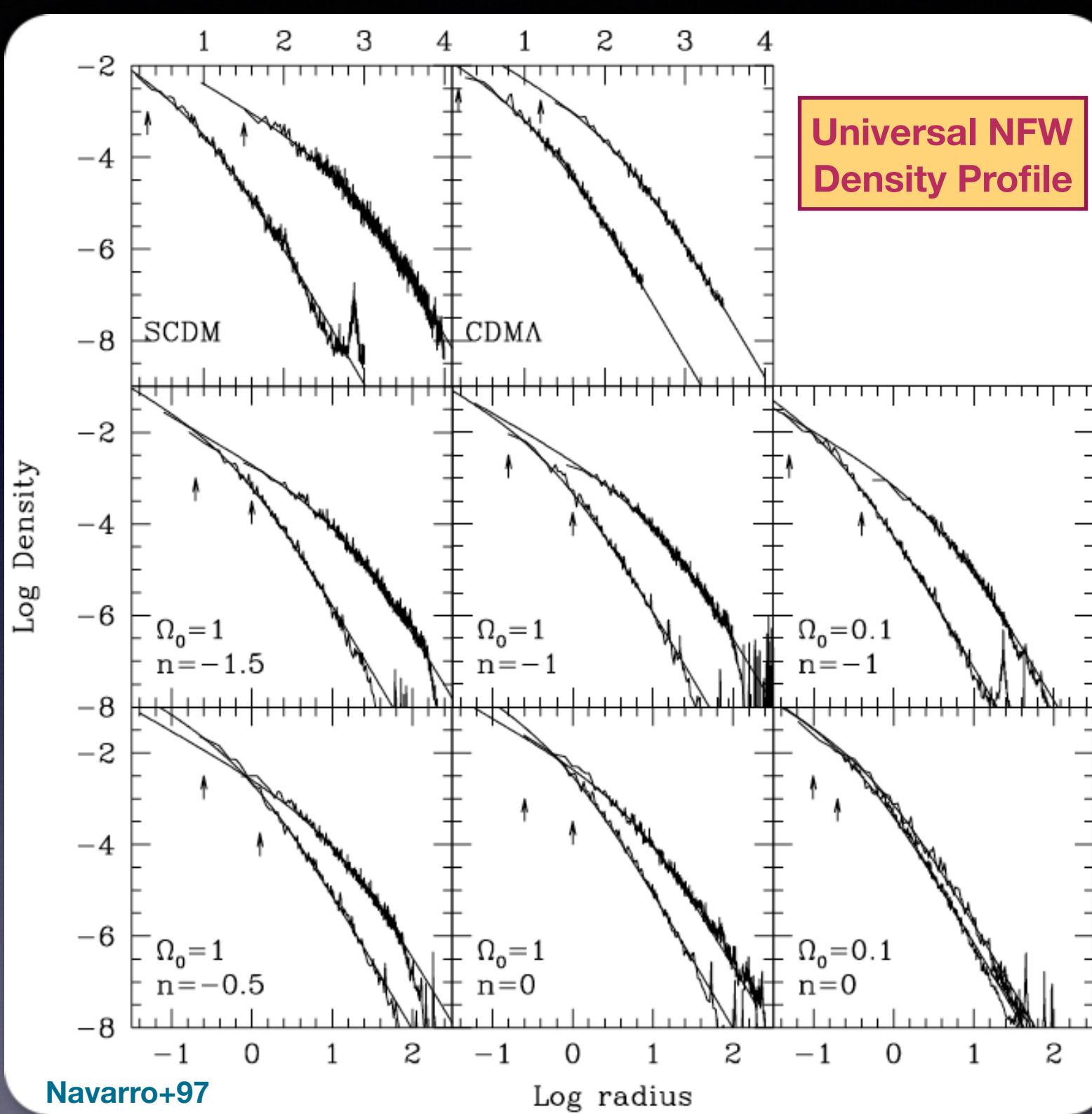
Large Scale Structure: CDM vindication



Non-Linear Matter Power Spectrum



Abundance & Structure of Dark Matter Halos



Cosmological N-body Simulations

What follows focusses exclusively on **collisionless** dark matter

Goal of simulations is to solve the **Vlasov-Poisson equations**, describing the evolution of **collisionless** system.

In N-body simulations, matter field is represented by set of **N** discrete particles. These do not represent physical objects. Rather they represent phase-space elements sampling the DF $f(\vec{x}, \vec{v}, t)$.

- Simulation is typically performed over a finite, periodic volume $V = L^3$.
- Simulations have finite mass resolution: $m_p = \bar{\rho} V / N$
- Simulations have finite force resolution, ϵ , which is required to suppress two-body collision effects.
- Initial conditions typically only sample modes of the power spectrum below the particle Nyquist frequency $k_{\max} = \pi/d$ $(d = L/N^{1/3})$

How to Test Simulations?

- Ideal: simulate systems for which you have an analytical solution
very rare in non-linear structure formation...
- Compare simulations against simulations
convergence; a necessary condition, but not sufficient...
different quantities (halo mass function, matter power spectrum, halo density profile, subhalo mass function, etc) all converge differently.

cross-correlation:

$$K = \frac{\langle \delta_1 \delta_2 \rangle}{\sigma_1 \sigma_2}$$

(1 and 2 refer to different simulations
with different numerical parameters)

- Look for signatures of collisional relaxation

- mass segregation (use ≥ 2 particle species with different masses)
- creation of isothermal cores in dark matter halos

Force Softening & Discreteness Effects

A ‘natural’ choice for ϵ is the mean interparticle separation $d=L/N^{1/3}$

In what follows, ϵ is normalized to d ($\epsilon=\epsilon/d$)

Modern ‘high-res’ codes (P^3M , tree-codes, AMR) typically use $\epsilon \sim 0.01-0.03$

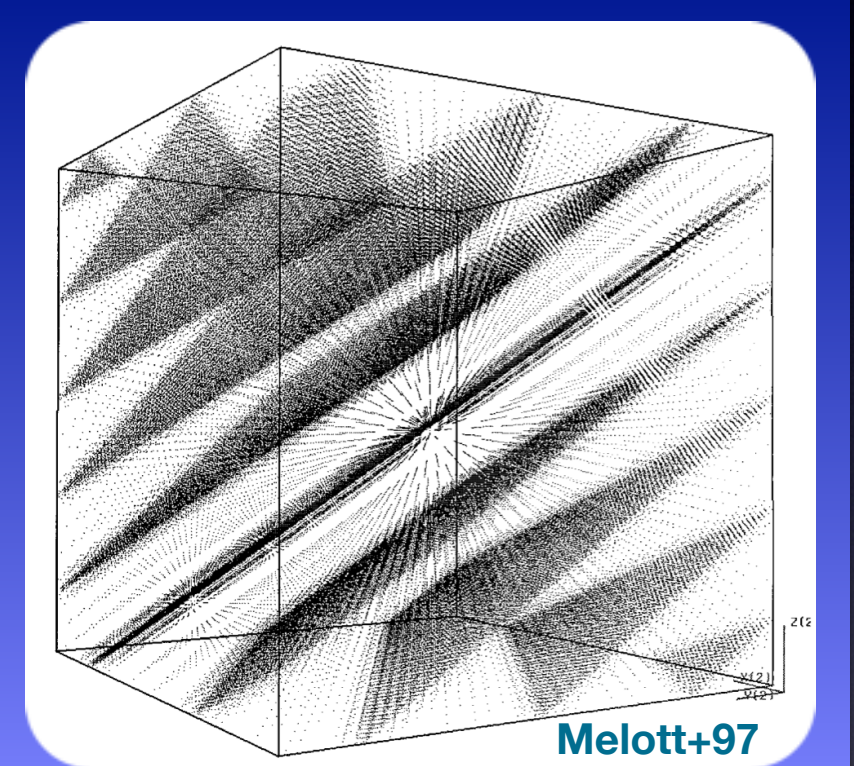
Efstathiou & Eastwood (1981):

P^3M simulations become collisional
(i.e., reveal mass segregation) if $\epsilon<0.1$

Peebles (1989): PM codes require $\epsilon \sim 1$

Melott et al. (1997):

N-body codes in general require $\epsilon \sim 1$



Lively, ongoing debate whether simulations with $\epsilon < 1$ are reliable...

(Kuhlman+96; Splinter+98; Knebe+00; Melott 07; Romeo+08; Joyce+09; Benhaim+16; Power+16)

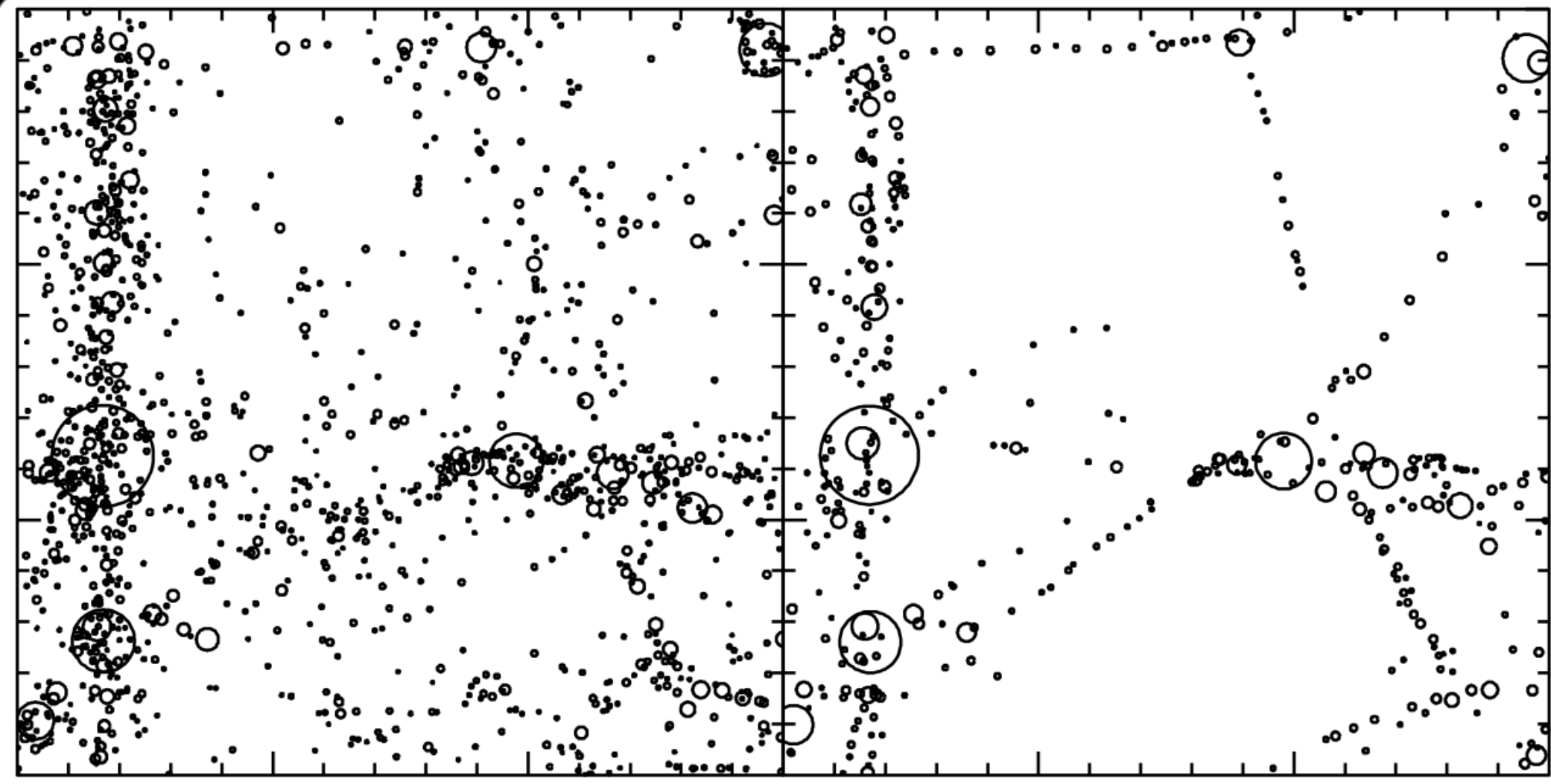
What is the optimal softening length?

(Athanassoula+00; Dehnen 01; Power+03)

At the very least, softening should be adaptive...

(Iannuzzi & Dolag 11; Hobbs+15)

Spurious Fragmentation

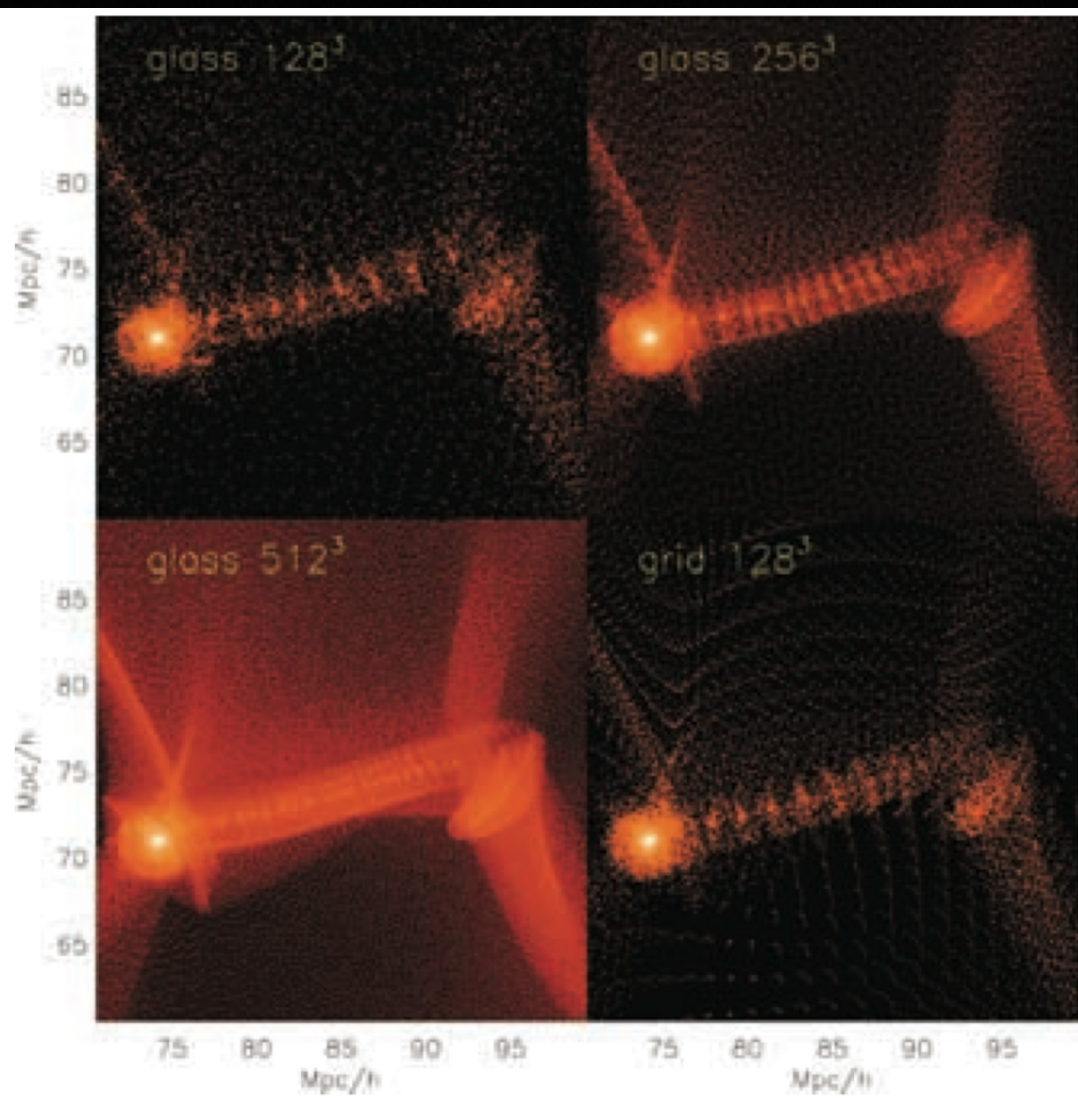


Warm Dark Matter simulations show 'beats-on-a-string' halos within filaments. These structures form on scales smaller than cut-off scale in power spectrum.

(Bode, Ostriker & Turok 2001; Knebe+02)

Initially interpreted as due to (physical) fragmentation (Knebe+03)

Spurious Fragmentations



Beats-on-a-string halos are manifestation of **spurious fragmentation**.

Spacing of artificial halos equal to grid-spacing.
Suggests link to regular, cubic lattice used for the initial particle load...

(Götz & Sommer-Larsen 2002, 2003)

But, spurious fragmentation also present with **glass-like** initial particle load, which has no preferred direction, and no long-range order.

(Wang & White 2007)

Source: Wang & White 2007

Spurious fragmentation now understood as arising from **discreteness-induced** velocity perturbations during early highly-anisotropic phase of structure formation

(Hahn & Angulo 2016; Power+16)

This is exactly the artefact that has been discussed again and again, since 1990, by **Melott, Shandarin** and collaborators!!

(see also Romeo+08; Joyce+09; Benhaim+16; Power+16 and references therein)

COMMENT ON “DISCRETENESS EFFECTS IN SIMULATIONS OF HOT/WARM DARK MATTER” by J. Wang & S.D.M. White

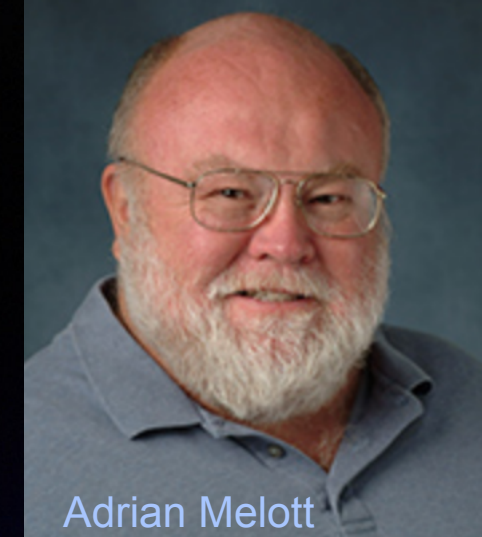
Adrian L. Melott, Dept. of Physics & Astronomy, University of Kansas; melott@ku.edu

ABSTRACT

Wang and White (2007) have discussed some problems with N-body simulation methods. These problems are a special case of a more general problem which has been largely unacknowledged for approximately 25 years, and affects results of all dark matter simulations on small scales (the definition of “small” varying with time).

They present results of a hybrid Tree-PM N-body simulation of hot/warm dark matter-dominated universes, which should have essentially zero initial fluctuation power on a fairly large free-streaming scale dependent upon the dark matter candidate. They analyze the spurious fragmentation of structures on smaller scales comparable to the mean comoving interparticle separation in the simulation. They conclude that such simulations are inaccurate on or below the mean interparticle separation, for both lattice or glass initial conditions.

I emphasize that this result is not restricted to such dark matter candidate models. The mass discreteness limitation has long been described in application to these models, as well as for models with initial power on small scales such as Cold Dark Matter (CDM). Extensive numerical experiments with multiple types of N-body codes have demonstrated that spurious fluctuations due to particle discreteness grow rapidly even in the presence of substantial small-scale power from the intended model spectrum, and modify the results on scales smaller than the mean comoving interparticle separation. This implies that the spatial resolution of such simulations is typically limited not by the force softening length, often referred to as the “resolution”, and not by the particle density in halos. Instead it is approximately $N^{-1/3}$, where N is the mean particle density, and of course depends on and improves very slowly with increased number of particles.

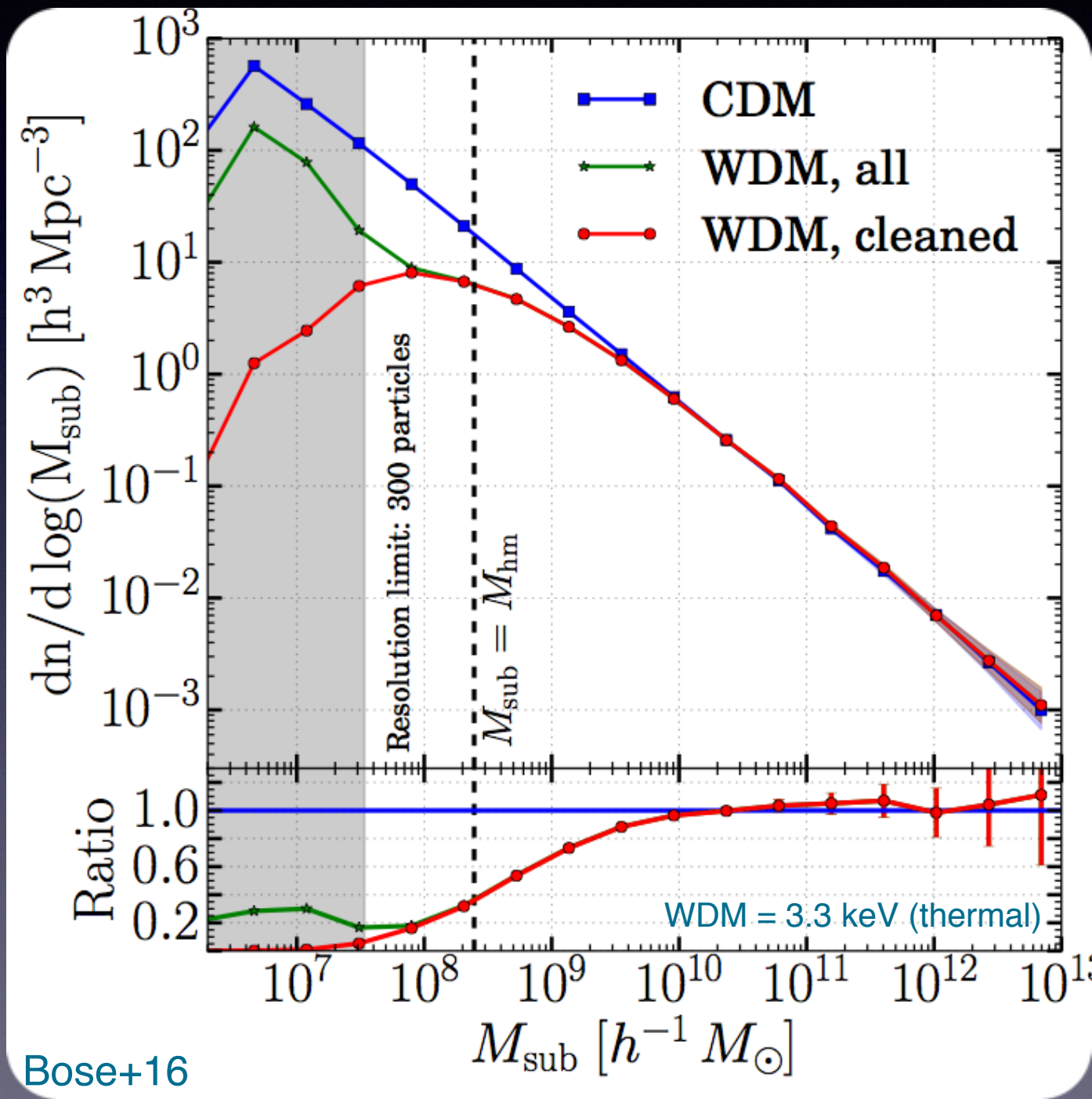


Adrian Melott

(Melott 2007; arXiv:0709.0745)

Testing the Nature of Dark Matter

Abundance & demographics of dark matter substructure depends sensitively on nature of dark matter: CDM vs WDM vs SIDM



Different models mainly differ in abundance of low mass halos, where galaxy formation is expected to be suppressed due to re-ionization.

WDM simulations suffer from artificial fragmentation; cannot be avoided.

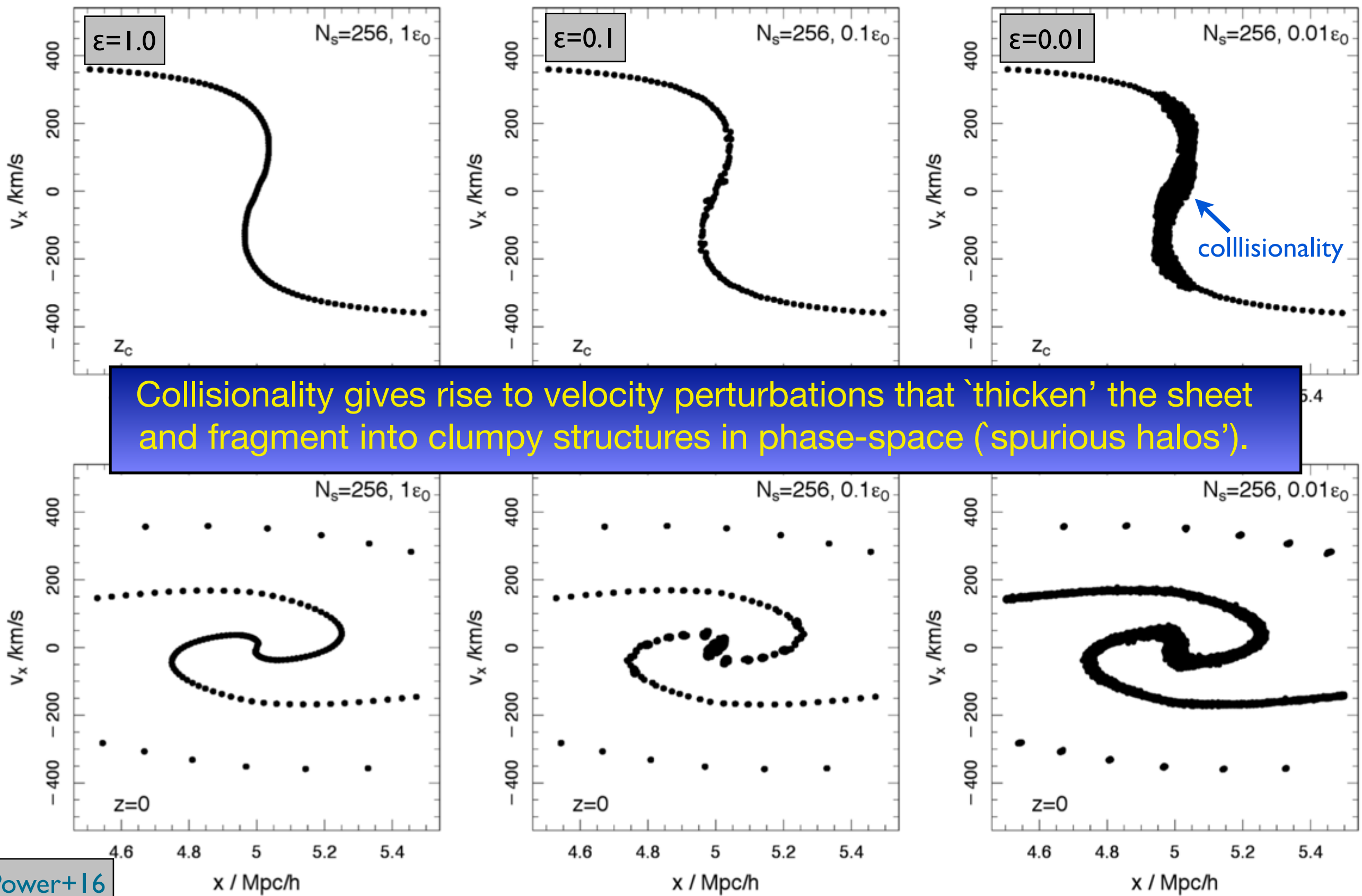
State-of-the-Art ‘solution’:

remove spurious halos ‘by hand’

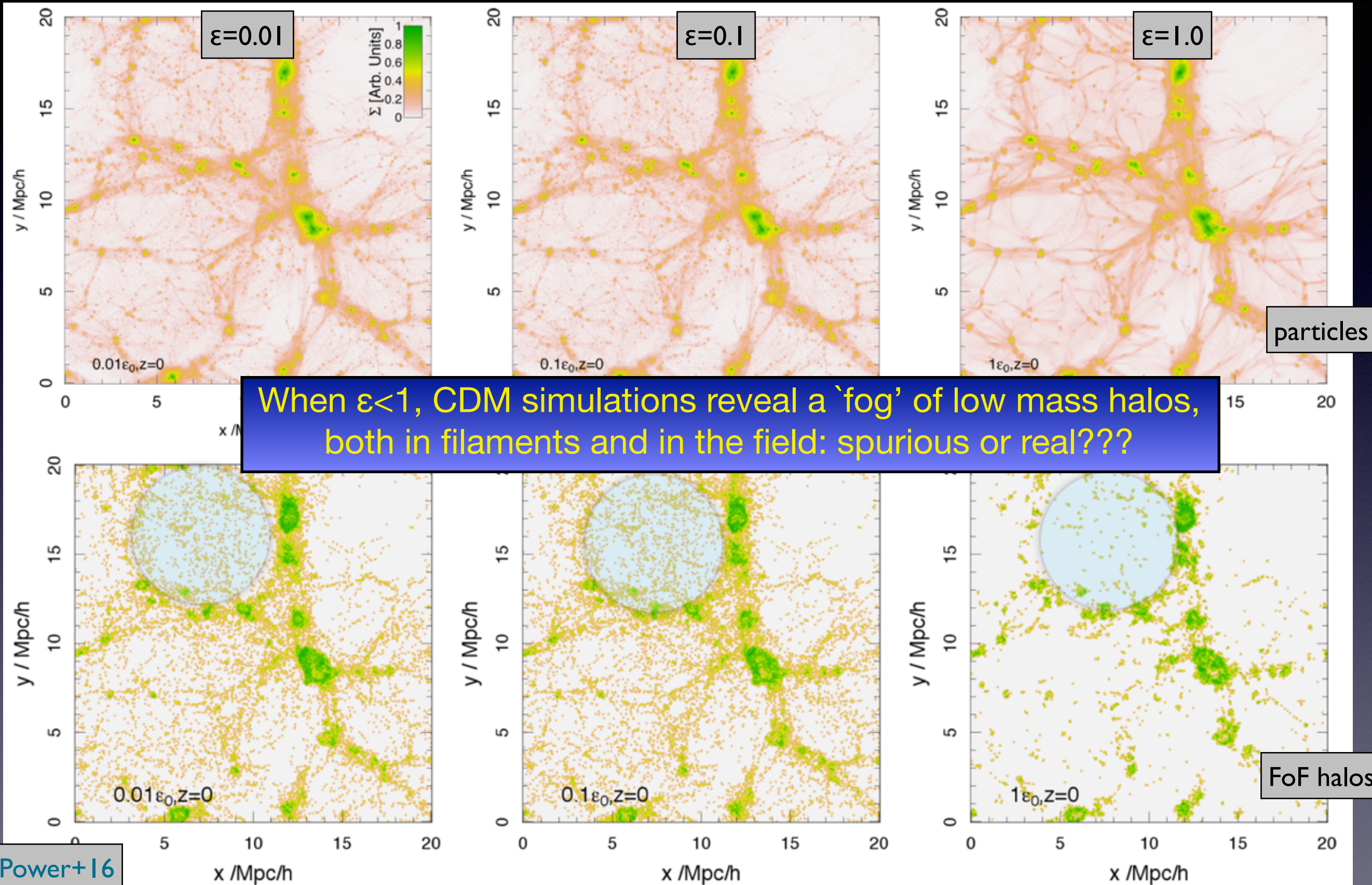
(e.g., Schneider+13; Lovell+14; Bose+16)

If spurious fragmentation is an outcome
of discreteness relaxation, shouldn't it
also be present in CDM simulations?

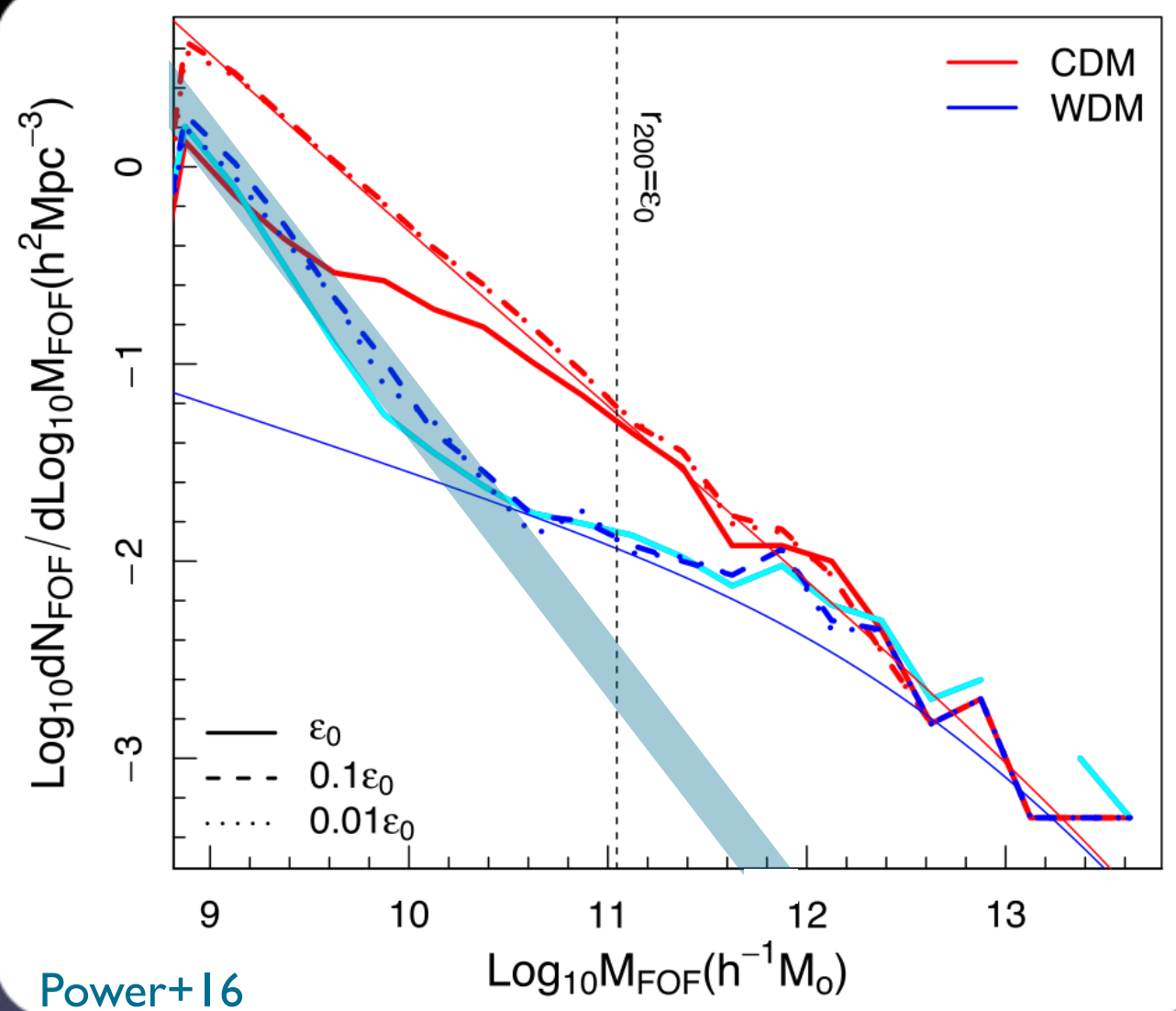
Plane-Symmetric Collapse



Spurious Fragmentation in CDM



Spurious Fragmentation in CDM



optimist's view

CDM does NOT suffer from spurious fragmentation, because

- no upturn, as for WDM
- agreement with EPS-predictions
- convergence; running at higher force resolution yields consistent results...

reality check...

BUT: WDM results have also converged.
But converged to garbage....

Why would spurious fragmentation not occur, or not matter, for CDM?

My
View

- It does happen, with similar abundance of spurious halos as for WDM
- Real halos dominate \gg no significant impact on CDM mass function
- But what about internal structure of halos? Is NFW reliable?

Two-Body Relaxation

Chandrasekhar (1943) derived change in orbit by summing over all (independent) two-body scatterings with all other particles in homogeneous system.

Roughly equal contribution from every decade in impact parameter:

$$\Gamma_{\text{relax}} \propto \frac{\ln \Lambda}{N}$$

$$t_{\text{relax}} \simeq \frac{N}{8 \ln \Lambda} t_{\text{cross}}$$

$$\Lambda = \frac{b_{\max}}{b_{\min}}$$

$$b_{\min} = b_{90^\circ} \simeq \frac{2Gm_p}{\sigma^2}$$
$$b_{\max} = L$$

Two-body relaxation generally deemed unimportant, since $t_{\text{relax}} > t_H$, for $N \gtrsim 100$

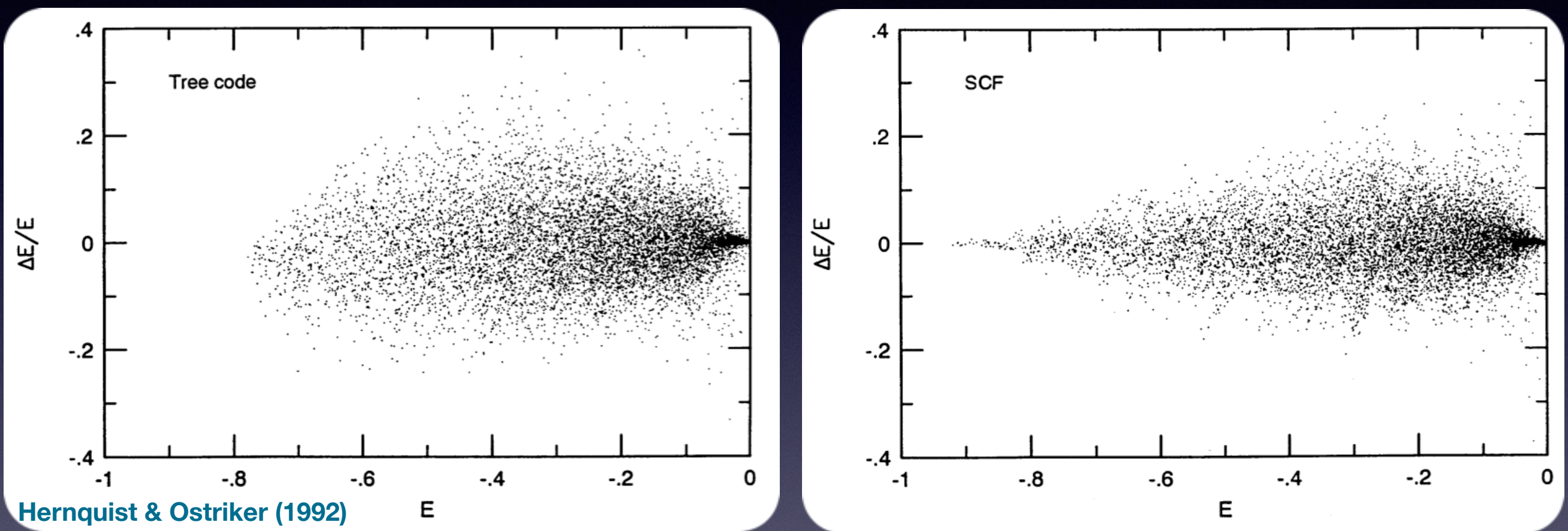
This ‘standard’ treatment of relaxation ignores three important points:

- each halo starts out small, when it is subject to severe relaxation
- orbits are quasi-periodic, giving rise to resonant effects
- self-gravity of large-scale fluctuations

[responsible for spurious fragmentation]

Discreteness Driven Relaxation

Self-Consistent Field (SCF) method, which uses basis-functions to compute gravitational potential (no softening required) suffer from same amount of relaxation as regular N-body codes (e.g, tree-code)!!



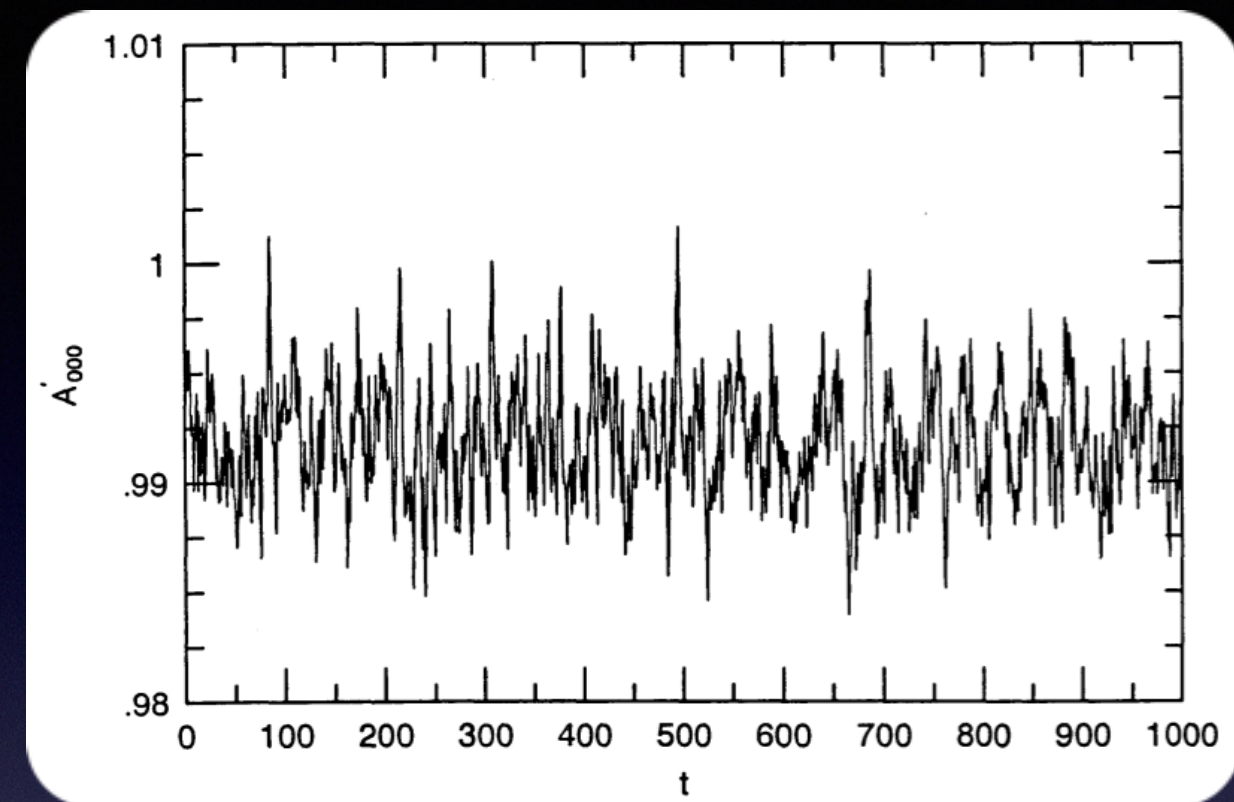
Dominant contribution to relaxation arises from non-local, collective modes of order the size of system in question.

(Weinberg 1993)

Discreteness Driven Relaxation

Poisson fluctuations cause fluctuations in large-scale potential, which drives relaxation (akin to violent relaxation).

In SCF method, this is evident from rapid fluctuations in the amplitude of zero-th expansion coefficient.



Source; Hernquist & Ostriker (1992)

Weinberg (1993): during the initial collapse phase, Poisson fluctuations may contribute relaxation that is factor 10-100 larger than what is predicted by local (i.e., Chandrasekhar) theory.

- Softening only suppresses impact of large-angle scattering events; not impact of small-angle scattering (large-impact parameters)
- Softening has little to no impact on these large-scale relaxation processes
- Only way to suppress these is by increasing number of particles

Discreteness Driven Relaxation

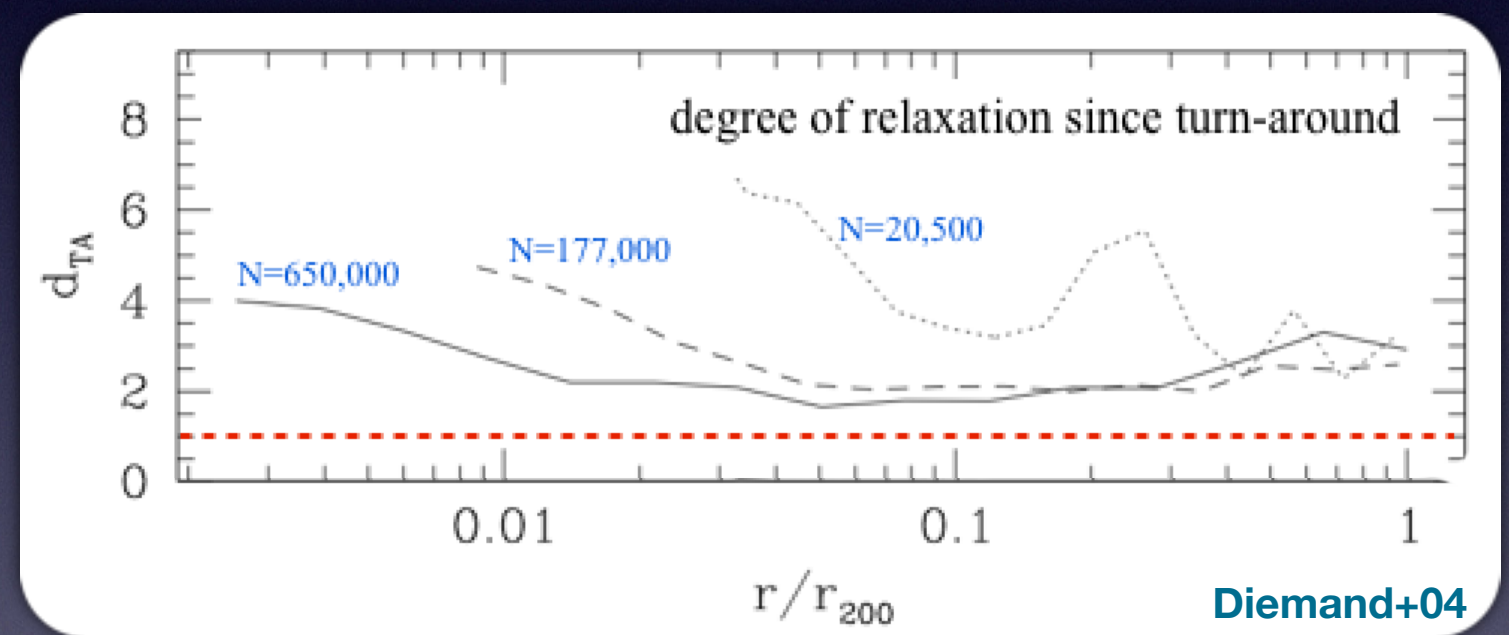
Progenitors of every halo start out small, and thus experience periods during which relaxation rate is large...

Fokker-Planck estimate

$$\Gamma_{\text{relax}} = \frac{G^2 m_p \rho \ln \Lambda}{\sigma^3}$$

$$d(t) \equiv \frac{\Delta E^2(t)}{E^2} = \int \Gamma_{\text{relax}}(t) dt = \sum_{i=1}^{N_{\text{step}}} \Gamma_{\text{relax}}(t_i) \Delta t$$

Diemand+04 integrated cumulative impact of relaxation for individual particles in cosmological N-body simulation.



Even in a halo with $N=650,000$ (at $z=0$), the cumulative relaxation is such that $|\Delta E| > E$

All knowledge about initial conditions has been erased due to two-body relaxation!!
And this doesn't even account for collective relaxation, which may well dominate...

A photograph of two puppets with orange, textured heads and white eyes. They are wearing dark brown suits, white shirts, and ties. The puppet on the left has grey hair and is speaking. The puppet on the right has white hair and is listening. They are set against a background of blue and white streaks resembling a galaxy or nebula.

Well, what
do you think of
simulations now?

I think they
are very relaxing

ASTR 610

The End